IMPACT STUDIES ON POLYETHERETHERKETONE (PEEK) - GRAPHENE COMPOSITES

By

SWETHA NARASIMHAN

A thesis submitted to the

School of Graduate Studies

Rutgers, The State University of New Jersey

In partial fulfillment of the requirements

For the degree of

Master of Science

Graduate Program in Materials Science and Engineering

Written under the direction of

Thomas Nosker

And approved by

_____

_____

_____

New Brunswick, New Jersey

October 2020

ABSTRACT OF THE THESIS

IMPACT STUDIES ON POLYETHERETHERKETONE (PEEK) GRAPHENE COMPOSITES

by

SWETHA NARASIMHAN

Thesis Director: Thomas Nosker

Graphene-reinforced polymer matrix composites offer high mechanical properties and have a wide range of potential applications including structural reinforcement materials, biomedical applications, packaging materials etc. The present study investigates the effect of the addition of graphene into the polyetheretherketone (PEEK) matrix. Graphene-reinforced polymer matrix composites (G-PMCs) were prepared using a high shear in-situ method with good particle-matrix adhesion of graphene at 2 wt.% and 35 wt.% in PEEK. The impact strength and the morphology of neat PEEK, 2% G-PEEK and 35% G-PEEK were characterized using Izod impact testing and by scanning electron microscopy (SEM). It was found that the impact strength of graphene reinforced PEEK is higher than neat PEEK at all degrees of exfoliation.

ACKNOWLEDGEMENT

First, I would like to thank God for giving me the strength to finish my thesis. I would like to express my sincere gratitude to my advisor, Prof. Thomas Nosker, for his steady support, guidance, and confidence he gave me through the years I was working in his group. His prompt inspirations, timely suggestions with kindness, and enthusiasm have enabled me to finish my thesis.

I want to express my thanks to the members of my committee, Prof. Richard Lehman and Prof. Deirdre O'Carroll, for their help and guidance. My completion of this project could not have been accomplished without the constant support and guidance of Arya Tewatia. I would like to thank Arya for the impact energy data and helping me with the SEM testing. I would also like to thank TLC Products Inc. for all their support. I also place on record my sincere thanks to all my lab mates and friends for their constant encouragement.

Lastly, I would like to dedicate my thesis to my family, whose support, understanding and patience have made me the person I am today. To my parents, Narasimhan and Meera Narasimhan, to my sister, Sneha Narasimhan, I will never be able to thank you all enough.

TABLE OF CONTENTS

LIST OF TABLES

LIST OF FIGURES

CHAPTER I

INTRODUCTION

Graphene is a single thin layer of carbon atoms arranged in a two-dimensional honeycomb lattice [1]. Recently, graphene has attracted both academic and industrial interest because it has been found that even a small addition of graphene has the potential to significantly increase the mechanical properties of a polymer matrix including elastic modulus, tensile strength etc. However, the improvement in the physicochemical properties of the composite depends on the process including extent of exfoliation, dispersion of graphene sheets, distribution and alignment in the polymer, and also the interfacial bonding between the graphene layers and the polymer matrix [2]. A strong interfacial bond between the graphene platelets and polymer network is vital for effective reinforcement. Poor interfacial adhesion may lead to little stress transfer between the graphene platelets and polymer matrix, resulting in lower mechanical properties in the composite material. [3]

The large surface area of graphene sheets per unit mass with good properties makes it ideal to be used in polymers but can lead to the formation of irreversible agglomerates through van der Waals interactions. For this not to occur, graphene sheets must be exfoliated thoroughly and dispersed homogeneously in polymer composites [4].

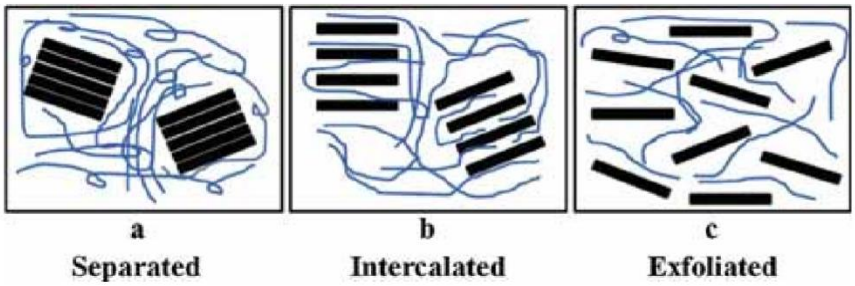

Figure 1 Different morphologies of polymer composites [5]

It has been found that graphene increases polymer impact toughness by inhibiting crack propagation [6], [7]. Graphene-polymer matrix composites (G-PMCs) can potentially be used in many industries such as aerospace, military, cars and planes. In such industries, the composite parts may be subjected to vibration which may lead to delamination of the composite and thereby the failure of the part [8]. However, the impact strength of the composite can depend on various factors like the crystallinity of the polymer, changes in the energy-absorbing mechanisms, creation of voids and crazes at the reinforcement edges, crack branching and bridging of any stress induced crack [9].

Polyetheretherketone (PEEK) is an organic colorless, semi-crystalline, and a high-performance thermoplastic engineering polymer in the polyaryletherketone family that sustains mechanical properties at high temperatures [10]. PEEK polymers are synthesized by step-growth polymerization by the dialkylation of bisphenolate.

PEEK-based composites are used in a wide range of industries including aerospace, chemical, biomedical, and automotive, due to the high mechanical properties, chemical inertness, and high temperature resistance of PEEK. The addition of nanoparticles to

PEEK increases friction and wear properties [11] and the addition of carbon or glass fibers to PEEK enhances mechanical properties especially stiffness [12], [13].

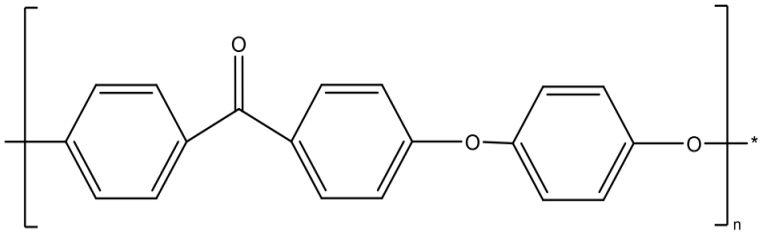

Figure 2 Chemical structure of PEEK [10]

The addition of carbon nanotubes (CNTs) to PEEK has been well studied. It was shown that the resulting CNT-PEEK composite has higher tensile modulus, higher thermal conductivity and higher electrical conductivity than the virgin PEEK [14]–[16]. However, few studies have been reported on G-PEEK composites.

In this investigation, G-PMCs is produced by a unique in-situ process where graphene layers are exfoliated from graphite in liquid polymers. G-PMCs have graphene-nanoflakes that are evenly distributed in and strongly bound to the polymer matrix. This method of mechanically exfoliating graphite to produce G-PMCs is easy to make and cheaper than the other methods. The resulting G-PMCs are light weight and also have a good stiffness.

In this experimental thesis, the impact strength of G-PEEK composites was explored and the morphology of the composites has been presented.

CHAPTER II

BACKGROUND

2.1 POLYMERS

Polymers are macromolecules built up by linking together large numbers of much smaller molecules (monomers) by forming chemical bonds. Depending on their structure, they can be classified as linear, branched, or crosslinked polymers. Polymers play a significant role in every aspect of modern life, such as health care, food, information technology, transportation, energy industries, etc. The speed of developments within the polymer industry is phenomenal and, at the same time, crucial to meet the demands of life in the present and the future. Applications for polymers range from adhesives, coatings, painting, foams, and packaging to structural materials, composites, textiles, electronic and optical devices, biomaterials, and many other uses in industries and daily life. [17].

2.2 GRAPHENE

Graphene is currently the strongest material, the ultimate strength is 200 times greater than the best performing steel [18]. Graphene is composed of only covalently bound carbon atoms, but it is a 2D flat sheet rather than a rolled-up monolayer of carbon [19]. Graphene is one of the allotropes (diamond, graphite, fullerenes, and carbon nanotubes) of the carbon family. Graphene is a planar monolayer of sp^2 hybridized carbon atoms arranged in a two-dimensional lattice [20]. The side by side overlap of the unhybridized p electrons of the carbon atoms form the pi bond between the carbon atoms. Graphene has been viewed as the basic building block for graphitic materials of all other dimensionalities [21]. For

example, the fullerenes (buckyballs, 0-D carbon allotrope) can be envisioned to be made by wrapping a section of graphene sheet, the carbon nanotubes (CNTs, 1-D carbon allotrope) can be viewed by rolling graphene nanoribbon, and graphite (3-D carbon allotrope) can be made by stacking graphene sheets on top of each other and separated by a distance of 3.37 A˚ [22].

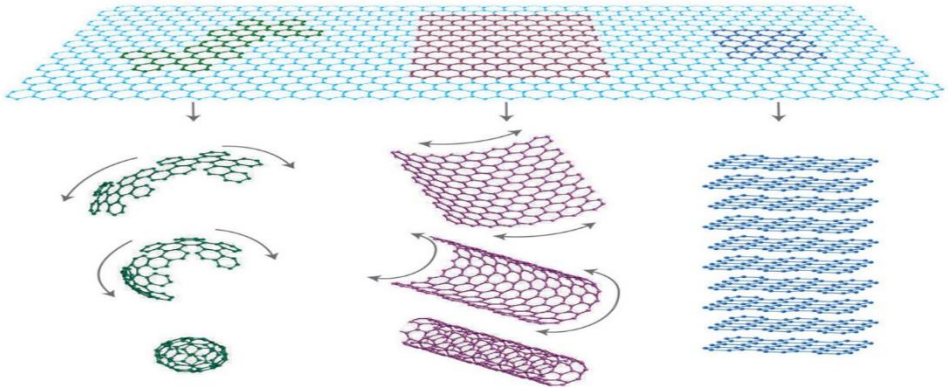

Figure 3 Graphene can be wrapped to form buckyballs, rolled to form CNT and stacked to form Graphite [21]

Graphene materials possess excellent characteristics of mechanical, electrical, and thermal properties benefiting from its sp^2 hybridization geometry. Graphene is used in many modern applications due to its properties. Few of the main properties are:

- The highest elastic modulus and high strength, 1 TPa and 130 GPa, respectively [23]
- Very high thermal conductivity, [24]
- High intrinsic electrical conductivity, [25]
- High specific surface area,
- Good optical transparency,
- High carrier mobility under ambient condition

Materials	Elastic Modulus (GPa)	Density (g/cm3)
Graphene	1000	2.267
Steel	200	7.75-8.05
Aluminium	69	2.71
Wood	8-11	0.5-0.8
PET	4	1.39
PEEK	3	1.31
HDPE	1	0.96

Table 1 Comparison of elastic modulus of different materials

Table 1 shows the elastic modulus of several different materials and it can be seen that graphene has the highest elastic modulus and polymers have the lowest. The specific modulus or specific strength of a material is the material's modulus or strength per mass density of the material. Aluminium alloys are used on airplanes because it is strong, stiff and has relatively low density when compared to steel. Due to the high elastic modulus and low density of graphene, Graphene composites have extremely high specific modulus and extremely high specific strength. Graphene composites may be used to replace aluminium due to their high specific modulus, strength, and they also have less density than aluminium.

Materials	Tensile Strength	Thermal conductivity (W/mk) at room temperature	Electrical conductivity (S/m)
Graphene	130 ± 10 GPa	4,840 – 5,300	On the order of 10^8
Carbon nano-tubes	60 – 150 GPa	3,500	3,000 – 4,000
Nano sized steel	1,769 MPa	526	1,350,000
Aluminium	300 MPa	205	38,000,000
Plastic (HDPE)	18 – 20 MPa	0.462 - 0.52	Insulator
Rubber (natural rubber)	20 – 30 MPa	0.13 - 0.142	Insulator
PET	50- 170 MPa	0.15 – 0.24	Insulator
Fibre (Kevlar)	3,620 MPa	0.04	Insulator

Table 2 Mechanical, thermal and electrical properties of various materials [2]

Let us consider a plastic PET water bottle. It can be easily deformed because of its low stiffness. But polymers are beneficial in terms of low density, high strength and being available at low cost. Composites are made in order to increase properties in polymers like stiffness, strength etc. Biaxially oriented PET has tensile strength almost equal to medium strength steel.

Table 2 gives a comparative chart on the mechanical, thermal and electrical properties of graphene with other materials like CNTs, steel, plastic and fiber. The tensile strength of graphene is similar or slightly higher than CNTs, but much higher than the other materials. Graphene has the highest thermal conductivity at room temperature when compared to other materials.

Graphene and its derivatives show tremendous potential in enhancing mechanical, thermal and electrical properties in various fields such as energy conversion, sensors, electronic materials etc. [19].

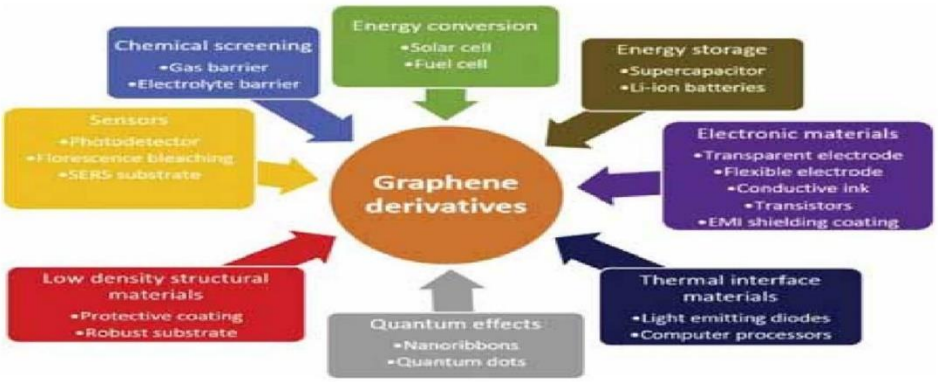

Figure 4 Various applications of Graphene derivatives [19]

2.2.1 HISTORY OF GRAPHENE

In 2004, two Russian researchers, Andrei Geim and Kostya Novoselov at the University of Manchester, were in an effort to explore properties of flakes of carbon graphite by making thinner flakes with the use of scotch tape. They used the scotch tape to peel off a layer of graphite and then continued to peel layer and layer from the flakes of graphite. They eventually found a material with unique and interesting properties which was one atom thick. The researchers had found graphene. It used to be thought that graphene couldn't exist in a layer. Later, their research was published and they were awarded the Nobel Prize in physics for their discovery.

2.2.2 PREPARATION METHODS OF GRAPHENE

Hummers method is used for producing graphene oxide (GO) (GO comprises of carbon, oxygen and hydrogen where there is a ratio of 2.1 and 2.9 of carbon to oxygen) through the addition of potassium permanganate to a solution of graphite, sodium nitrate, and sulfuric acid. This step is followed by addition of hydrogen peroxide which reduces residual permanganate. Ultra-sonication is then carried out to get monolayer of GO. This method is modified further to obtain graphene, by the addition of certain reducing agents such as hydrazine or sodium borohydride. However, the reduced graphene sheets have defects because of the reduction process due to which the properties of graphene may not be utilized to its highest potential. Furthermore, the chemicals used in this process are hazardous due to which the commercialization of graphene is hindered. Due to the above-mentioned reasons, the production of graphene from graphene oxide is expensive [26].

Another method of preparation of graphene is Chemical Vapor Deposition (CVD). This method uses carbon-rich precursors like methane and recombines the carbon atoms on the surface of metal foil (Nickel or Copper) in an inert atmosphere at over 1000^{o}C [27]. Single, double or multiple layer graphene with various sizes can be obtained by changing the reaction parameters, such as the ratio of the different precursors, temperature, and substrates. However, CVD synthesis can result in heterogeneous and defective structures [19].

2.3 COMPOSITES

Composites are a combination of 2 or more chemically distinct and insoluble phases. Composites involve of one or more discontinuous phases (reinforcement) embedded in a continuous phase (matrix). The matrix can be polymers, metals, ceramics, or carbons.

Composites are heterogeneous at the macro level. They can be defined as either quasi or locally homogeneous if fibers are regularly spaced [28]. Composites have a wide range of applications due to its innumerous advantages such as high specific strength, low thermal conductivity, low coefficient of thermal expansion [29].

Polymer micro composites became a significant part of polymer science and engineering because people could make compositions that had properties unattainable with homopolymers, like, for example, higher specific modulus. Polymer composites consist of a polymer or copolymer having particles dispersed in the polymer matrix. In recent years, polymer composites have attracted great interest because they often exhibit great improvement in materials properties at reasonable cost when compared to traditional and heavy materials like wood, aluminum and steel [10]. Polymer composites have existed for a long time, with glass fibers, carbon black, pyrogenic silica, and diatomite used as additives in polymers [17]. The properties of the conventional polymer are enhanced by incorporating particles into the polymer matrix, thus changing their electrical, mechanical, and thermal properties [30]. These enhancements can include high moduli, increased strength and heat resistance, decreased gas permeability and flammability, and increased biodegradability of biodegradable polymers [17]. Polymer composites can be used in many applications including boats, sporting goods, car bodies etc.

2.4 POLYMER GRAPHENE COMPOSITES

Polymer micro composites with exfoliated layered silicate fillers were developed [20], and nearly forty years later, a report showed significant mechanical properties (strength and modulus) improvement using clay as filler in a nylon-6 matrix [31], which attracted significant academic and industrial interest in composites. With the development of nanoscience and technology, many nanofillers, such as carbon black, nano-silica, CNTs, carbon and glass fibers have been widely studied and used to enhance mechanical, thermal, electrical, and gas barrier properties of polymers. One main disadvantage of using carbon fibers and CNT is the high production cost of carbon fibers and CNT. When carbon fiber and glass fibers are added to the polymer matrix, the mechanical properties such as stiffness and tensile strength enhances, the strain to failure goes down, the density increases and the impact strength decreases. The impact strength reduces because the fiber ends act as a point defect at fiber tips, while cracks can easily go around the fibers thus decreasing the amount of energy absorbed before fracture. Graphene has the potential to be used as a low-cost alternative because it can be derived from a low cost, graphite precursor available in huge quantities [3]. Since graphene has a higher surface-to-volume ratio than CNT because of the inaccessibility of the inner nanotube surface to polymer molecules [32], graphene is promising to be more favorable for enhancing the properties of polymer matrices. Also, graphene offers more advantages towards highly improving mechanical properties including strength and stiffness in the polymer composites because their planar structure and high aspect ratio are expected to endow better stress transfer from graphene particles to the matrix while loading [33]. One might expect impact strength to drop when graphene

is used as a nanofiller because that's what happens with all the other fibers, including carbon fiber and glass fiber.

Generally, traditional preparation methods of polymer graphene composites start with graphite being turned to graphene through solution-based processing, melt-based processing, chemical grafting, latex emulsion blending, layer-by-layer assembly and directed assembly [34]. Once the graphene is obtained, it is then dried and mixed with polymers in an extruder in order to prepare polymer graphene composites. In the previous few years, graphene and its derivatives have been incorporated into a wide range of polymers including epoxy, polystyrene (PS), polypropylene (PP), polyethylene terephthalate, polyaniline (PANI), nylon and polymethylmethacrylate (PMMA) for several functional applications [35].

Figure 5 depicts a stress-strain curve showing various mechanical properties such as 1) Elastic modulus or stiffness which is the resistance to elastic deformation shown by the slope of the stress-strain curve, 2) Yield strength which is the maximum stress that can be applied before plastic deformation, 3) Ultimate tensile strength which is the maximum stress that a material can withstand while being stretched prior to breaking, 4) Strain to failure, 5) Toughness which is the maximum amount of energy absorbed prior to failure. A tough material can withstand high stress under maximum elongation and toughness can be evaluated by calculating the area under the stress-strain curve. Numerous applications require high toughness, thus maintaining a balance between high tensile strength and elastic modulus.

The addition of stiff nanofillers results in high mechanical strength and elastic modulus but lower elongation therefore lower toughness. It is nearly impossible to obtain a composite material with high elastic modulus, high tensile strength, high elongation and high toughness [36]. Thus, one of these factors is improved depending on the applications of the composite material.

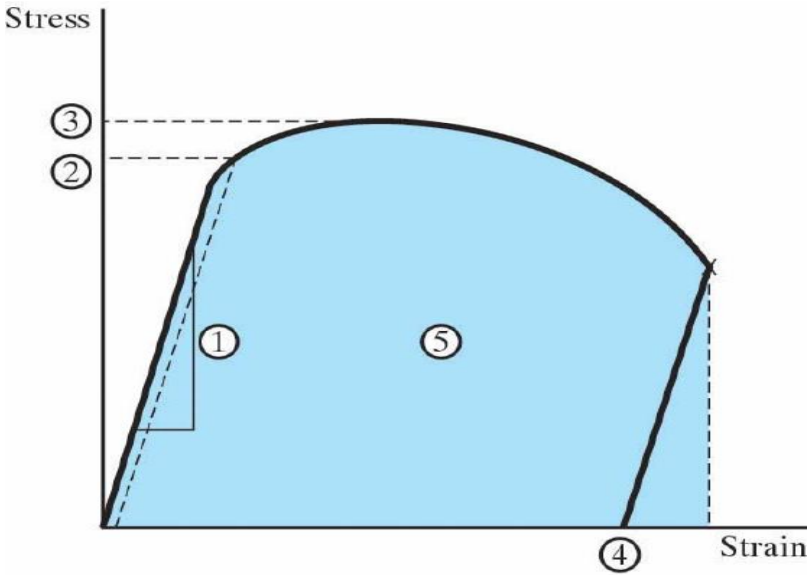

Figure 5 Stress-strain curve [37]

2.5 INTERFACE OF POLYMER COMPOSITES

The overall performance of the composite is highly dependent on the interface and the immediate contact surfaces between the reinforcing phase and the bulk phase. The interfacial adhesion between the reinforcing phase and the bulk phase of the polymer composite and covalent bonding at edges play a significant role in the stress transfer from the bulk phase to the reinforcing phase. The better the interfacial adhesion, the greater the load the composite can withstand before failure, and the greater the mechanical properties of the polymer composite. On the other hand, lower interfacial adhesion leads to lower load transfer between the bulk and the reinforcing phase and thus resulting in lower strength of the polymer composite. Thus, strong interactions between the reinforcing phase and bulk polymer are essential for high strength of the polymer composite [38]. Different possible bonding opportunities between graphene and the polymer matrix are covalent or primary bonding and secondary bonding because of the high surface area of graphene. When graphene sheets are ripped apart free radicals are produced which provide covalent bonding opportunities. Pi bonds on the surface of the graphene sheets provide secondary bonding opportunities. Interfacial interactions between the polymer-filler interface enable the slippage mechanism to be activated resulting in higher toughness [19]. Graphene is an ideal nanofiller component because graphene is not only mechanically strong but also flexible thus resulting in composites with high impact toughness [2], [32].

2.6 MECHANICAL PROPERTIES OF GRAPHENE POLYMER COMPOSITES

2.6.1 FROM TRADITIONAL GRAPHITE TO GRAPHENE METHODS

Jeffrey et al. presented a report of polymer composites using microwave exfoliated graphene oxide (MEGO) as filler. MEGO is a high surface area carbon material which can be sheared apart during melt mixing with a polymer host. Graphite oxide (GO) was prepared via a modified Hummer's method and then was dried for 48 hours in the presence of vacuum. Subsequent to drying the GO was loaded into a glass beaker and then put into a domestic microwave oven and heated for about 20 seconds to cause rapid exfoliation and reduction of the material to form MEGO. The polymer and MEGO powder were fed into a twin-screw micro compounder with a mixing chamber volume of 5 ml, mixing temperature of 250^{o}C and a residence time of 9 minutes.

In this report, dynamic mechanical analysis (DMA) was used to evaluate the mechanical properties of the composite material. Figure 6 depicts the storage modulus of neat polycarbonate and various loadings of MEGO-polycarbonate composite materials [39].

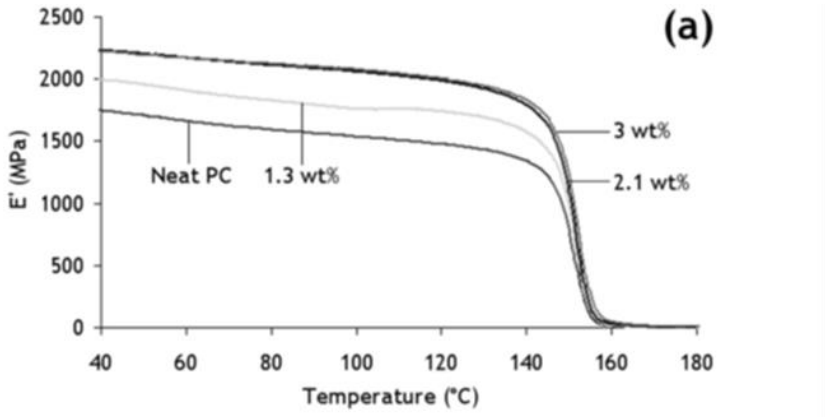

Figure 6 Increase in stiffness for Polycarbonate based Graphene composites in Other labs [39]

We can see a 14% increase when 1.3 wt.% of MEGO is added to the polycarbonate matrix and a 28% increase when 2.1 wt.% and 3 wt.% MEGO is added to the polycarbonate matrix [39].

Naebe et al. experimentally investigated the mechanical properties of covalent non-functionalised graphene/epoxy nanocomposites and functionalised graphene/epoxy nanocomposites. In this experiment, graphene oxide (GO) was prepared using natural flake graphite in a solution of nitric acid, sulphuric acid and potassium chlorate for 96 hours. The GO was further dried in a vacuum oven and the vacuum dried GO was placed in a quartz tube which was then inserted into a Lindberg tube furnace for 30 seconds to obtain thermally reduced graphene [40]. Further, thermally reduced functionalized graphene was produced using Bingel reaction and the Bingel modified graphene was incorporated into epoxy resin. Graphite nanoplatelets were dispersed in acetone using a probe sonicator for 30 minutes. Then, the epoxy resin was added and the suspension was ultrasonicated for one more hour. The above mixture was heated at 70^{o}C for 8 hours to remove acetone. It was then added into a preheated teflon mould and cured in an oven at 120^{o}C for 2 hours in order to produce composite samples. This was followed by a post curing step at 177 ^{o}C for 2 hours.

Figure 7 shows the change in flexural modulus and flexural strength upon the addition of graphene and functionalised graphene to epoxy resin. We can see a 15% and 22% increase in flexural modulus when non-functionalised graphene and functionalised graphene is incorporated to epoxy resin respectively [41].

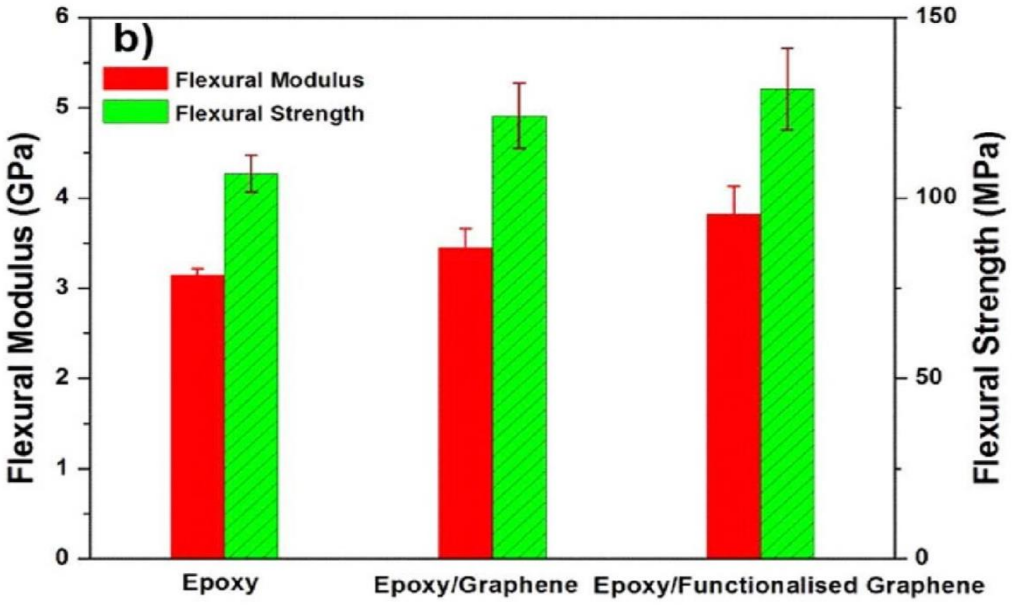

Figure 7 Increase in flexural properties for Epoxy based Graphene composites in Other labs [41]

Both the above experiments (Figure 6 and Figure 7) show a small percentage of increase in modulus. This is because of the weak secondary bonding between graphene and the polymer. The graphene present in the composite material has satisfied carbon valency thus resulting in weak interactions with the polymer matrix and thereby decreasing the mechanical properties improvement.

2.6.2 FROM IN-SITU EXFOLIATED G-PMCs

The present investigation provides a graphene-reinforced polymer matrix composite prepared by polymer processing methods comprising in situ exfoliation of well-crystallized graphite particles dispersed in a molten thermoplastic polymer matrix. Extrusion of a graphite-polymer mixture shears the graphite to exfoliate graphene sheets and enhances the mechanical properties of the bulk polymer [6].

Mechanical exfoliation of graphite within a polymer matrix may be obtained by a polymer processing method that imparts repetitive high shear strain events to mechanically exfoliate graphite microparticles into multi- or single-layer graphene sheets within the polymer matrix [6].

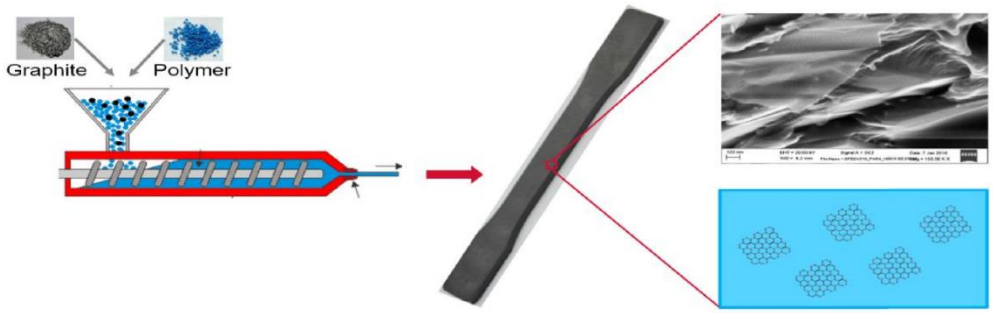

Figure 8 In-situ exfoliation of Graphite into Graphene

Figure 9 and Table 3 shows the tensile modulus of various polymers upon the addition of 35% graphene. The bars in blue indicate the tensile modulus of various neat polymers and the bars in orange indicate the tensile modulus when graphene is completely exfoliated into the polymer matrix.

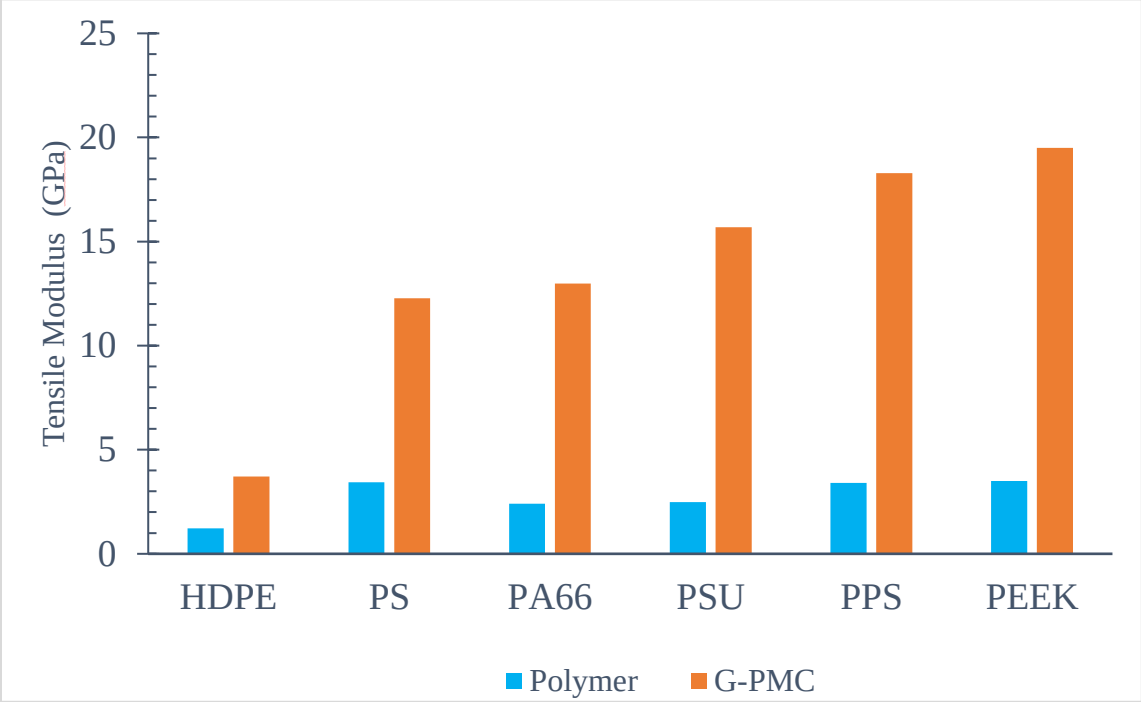

Figure 9 Increase in tensile modulus in various polymers

Polymers	Percentage increase in Tensile Modulus upon addition of 35% graphene
HDPE	200 %
PS	250 %
PA66	440 %
PSU	530 %
PPS	437 %
PEEK	460 %

Table 3 Percentage increase in Tensile modulus in our technology

We can see a significant amount of increase in tensile modulus upon addition of 35% graphene when G-PMCs were fabricated through in-situ exfoliation. While comparing Figure 7, 8 and 9 we can see that graphene polymer matrix composites made from in-situ exfoliation of graphite has shown the highest increase in modulus upon addition of graphene. The in-situ exfoliation process led to formation of free radicals of graphene which creates opportunity for primary bonding i.e. covalent bonding with the polymer matrix upon mechanical exfoliation and thus leading to better stress transfer between graphene and the polymer matrix.

2.7 DRYING TIME OF POLYMERS

Almost all commercial polymers will absorb a certain amount of moisture from the atmosphere and even a small amount of moisture can cause degradation issues when the material is heated. This is particularly the case for condensation polymerized polymers. While some polymers only need to have surface moisture removed, others need all moisture to be removed such as the condensation polymerizable polymers. When heated, each single water molecule present in the condensation polymerizable polymer tends to break the covalent bonds in the polymer, reducing the molecular weight of the polymer. Thus, polymers need to be dried before processing. Various type of dryers including dehumidifying dryers, rotary wheel dryers, low pressure dryers or vacuum dryers, compressed air dryers and hot air dryers can be used for drying of polymers.

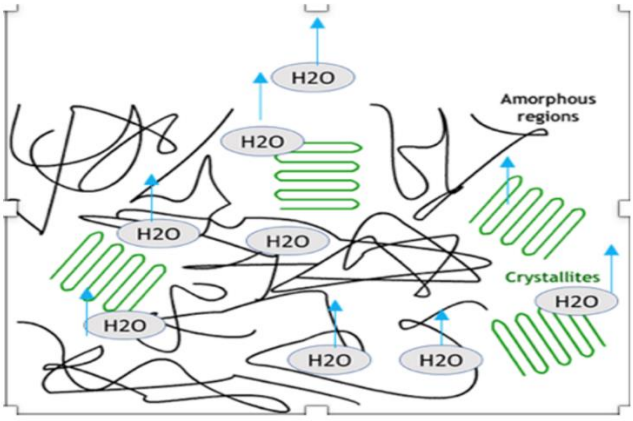

Figure 10 Drying in Polymers

Drying time and temperature for PEEK is 150^{o}C for 3 hours or 120^{o}C for 5 hours.

2.8 DRYING TIME OF G-PMCs PELLETS PRIOR TO MOLDING

The process of exfoliating graphene from graphite involves shear stresses imparted by the liquid polymer to the graphite, peeling the layers of graphene from the graphite, creating new surfaces, and also ripping the graphene sheets. If we consider a simple model to explain things, we start with mined graphite which is separated using a 300-micron screen. Consider a simple case of a cube of graphite 300 microns on a side, which is about the size of a grain of salt. This would be made up of a million layers of graphene, and each sheet of graphene would have an area of 90,000 square microns (300 µm * 300 µm). When we look at broken graphene-polymer composites, we find that graphene sheets are broken into much smaller sheets of diameter close to 10 – 15 µm.

If we assume plates of graphene are all 10 microns, then from only one particle of graphite at the start, we get 1,000,000 sheets, which are each torn into 900 sheets of graphene, yielding 900 million sheets of graphene.

We can load many such graphite particles per polymer composite bead, yielding many billions of graphene sheets per pellet, which is an interesting proposition. For one thing, there can be great bonding, both primary and secondary. For another, drying will necessarily take extra time, and any effort to estimate dryness quickly (as is the case with typical moisture balance tests) will yield an erroneous result. Higher loading will also affect drying time.

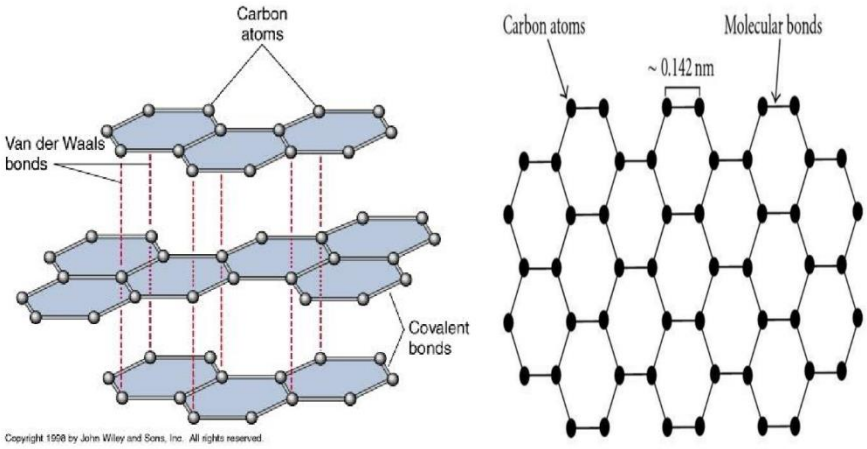

Figure 11 Graphite (left) to Graphene (right)

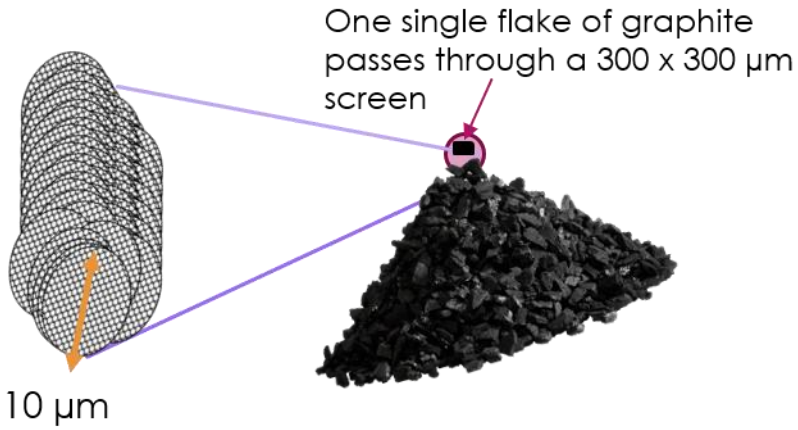

Figure 12 Magnified image of a single graphite particle

While some polymers only need to have surface moisture removed, others need all moisture to be removed such as the condensation polymerizable polymers. The water molecule can break the covalent bonds between the polymer when heated which decreases the molecular weight and thus significantly decreasing the mechanical properties of the G-PMCs, especially strength-related properties. This effect can typically be avoided by drying the G-PMCs at least three times longer than the usual drying time of the virgin/neat polymer at the normal temperature (dependent on drying method) to remove the proper moisture content from the composite material. G-PMCs are novel materials that are different from the neat, host polymer; both in terms of chemical structure and morphology.

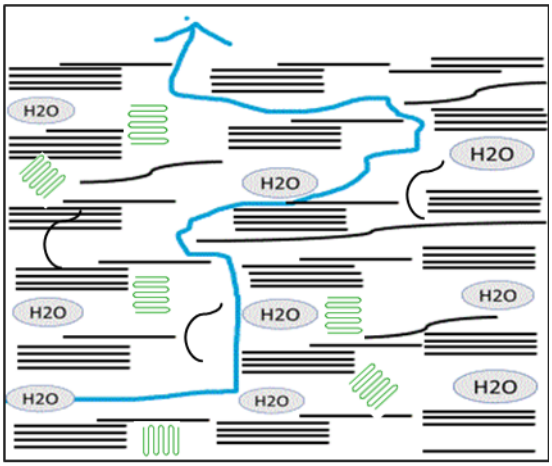

Figure 13 Drying in G-PMCs

In the case of G-PMCs, the path for a water molecule to travel is impeded by the many impermeable graphene layers, and thus, the path to escape from the pellet is much longer,

equal to several radiuses of the pellet. This has the practical effect of requiring more time to dry. The temperature to dry is determined by the polymer in question, so this should be consistent with recommendations. The fastest way to dry for laboratory experiments is usually in a vacuum oven.

Drying time and temperature for graphene reinforced PEEK is 9 hours at 150 ^{o}C or 15 hours at 120 ^{o}C which is three times the standard drying time for PEEK.

2.9 POTENTIAL APPLICATIONS OF GRAPHENE POLYMER COMPOSITES

- Structural reinforcement materials

The addition of even a small amount of graphene to the polymer matrix can increase the mechanical properties of G-PMCs thus indicating the use of these materials in various transport applications which requires the combination of high strength and lightweight like helmets, lightweight vehicles, aircraft, boats etc. Another developing application for G-PMCs has focused on sporting goods applications like cricket bats, knee pads, baseball bats, hockey sticks, tennis rackets, badminton rackets, golf sticks, archery arrow, skating boards, athletic cups, shin guards, shoulder pads etc. G-PMCs can also be used in infrastructure systems like mid-span bridges, tactical military bridges [20].

- Daily life applications

G-PMCs can be used in our daily life through many applications like book racks, luggage racks, furniture, storage containers and bins, shoe racks, mobile cases, bathtub furniture, mobile cases etc.

- Packaging materials

Another emerging application for G-PMCs has focused on packaging applications because of their improved barrier properties and better light absorption [42].

- Biomedical applications

G-PMCs may be used in many biomedical applications ranging from drug delivery and imaging due to their biocompatibility and their excellent properties [43].

Numerous other applications of G-PMCs include Construction hats, Automobile bumpers, Industrial shoes, Super strong body armor, Bags/Luggage, Windmill blades, Industrial pipes, Drones, Fishing rods, Door handles, Impact absorbers, Brake discs of airbus, Rocket motor, Turbine motor etc.

2.10 HISTORY OF IMPACT TESTING

The historical backdrop of impact strength testing dates to the nineteenth century. It was profoundly determined by the structure of the railroads when it was found that impact loads influence materials distinctively to static loads. During this time, the progress of impact strength testing was generally determined by the British. Rodman planned and made a drop weight machine which was utilized to test completed items like pipes and ankles in 1857. The weight was dropped on the materials and, it either broke or it didn't break. The information produced was utilized in the making of different products, and Rodman's machine was used for 30 years to test steel and other metal items [44].

However, Rodman was not the first one to make a documentation of impact strength testing. A man named Tredgold published a theory of cast iron to resist impact forces in 1824, which was indeed the first documentation of impact strength testing. The introduction of the notch on the samples improved the impact testing. Some plastic material just bent without breaking; however, with a notch, the material became more brittle due to which the improvement in impact testing was significant. National and international bodies like The American Society for Testing and Material (ASTM) and the International Association for Testing Materials (IATM) were responsible for establishing the standardization of impact strength tests between 1895-1922 [44].

One drawback of the drop weight machine was that it didn't give any information apart from whether the material broke or not. Later during 1898, Russell made a Pendulum impact machine that provided information on the amount of energy absorbed by the material when an impact force is applied. The machine was massive and thus could be used to break large products [44].

The ASTM developed many standard methods for the pendulum impact strength tests for metals between 1922-1933, and the Charpy and the Izod test were the two approved tests. The ASTM standards gave information regarding the geometry of the specimens, the size of samples, geometry of the striking edge and distance of striking, notch, and the dimensions of the hammer [44]. The two tests differ in the way the sample is supported [45].

2.11 IMPACT TEST

The pendulum impact strength test is a dynamic test in which a pendulum hammer of known mass is attached to the machine, and one swing of the hammer causes the specimen to fracture. Specimens used in this test may be notched or unnotched. The notched specimen increases the likely hood of specimen breaking with a brittle fracture rather than a ductile fracture because a stress concentration is produced at the notch [46], [47]. Also, both impact loading and the presence of a notch increase the probability of brittle fracture. The presence of notch also makes crack initiation easier under impact loads [45]. The two approved tests: the Charpy and the Izod tests also measured the bending impact strength of the specimen. The major factors that affect the results of an impact test are velocity, specimen, and temperature.

The impact test signifies the toughness of a material which denotes the amount of energy absorbed before fracture. Ductility is a measure of a material's ability to withstand stress without breaking, but just because a material is ductile does not mean that it is tough. A good combination of strength and ductility is the key to toughness. A material with high

strength and high ductility will have more toughness than low strength and high ductility. Strain rate, temperature and sensitivity of notch have a significant influence on the toughness of the material. The result of the impact test can also be used to study the strain rate [45].

2.11.1 IMPACT ENERGY

Impact energy is a measure of work done to fracture a test specimen [48]. When the swinging hammer hits the specimen, the specimen will absorb energy until it yields, and then the specimen plastically deforms at the notch. A fracture occurs when the specimen can no longer absorb energy [45].

Tougher materials will have a higher impact strength compared to brittle materials [48]. The purpose of the impact test is to measure a material's ability to resist loading.

The major factors that affect the impact strength of a specimen: -

- Temperature

The impact strength of the notched bars is dependent on temperature.

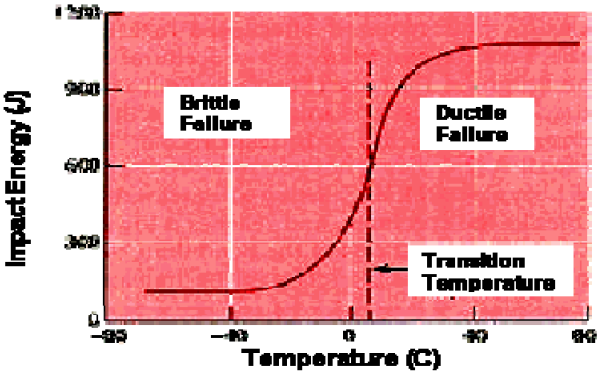

Figure 14 Effect of temperature on the Impact energy absorbed [45]

In some cases, below a particular temperature, the energy absorption is low, and brittle fracture occurs. In other cases, the failure is ductile, and energy absorption is much higher than the latter [45].

- Notch sensitivity

The presence of a notch raises the elastic limit of the material at the notch. When a crack is formed at the notch, the stress increases, and the crack quickly progress across the section. The advantage of the presence of a notch is that the total capacity to absorb energy can be detected and also makes failure more likely to occur [45].

- Velocity

For some materials, the speed at which the specimen is impacted by the hammer determines the type of fracture [49].

- Size of the specimen

Different sizes of specimens may allow different numbers of defects in the material which can act as stress risers and thus lower the impact strength of the material.

2.12 IZOD TEST FOR PLASTICS

The Izod impact test is an ASTM D-256, ISO 180 standard method used for measuring the impact strength of cantilevered notched specimens hit by a swinging hammer. The test is named after Edwin Gilbert Izod, who described it in 1903.

A notched sample is also used to determine notch sensitivity [45]. A range of pendulums having energies ranging from 2.7 J to 21.7 J may be used with most machines for testing of plastics.

2.12.1 SCHEMATICS OF THE IZOD TEST – ASTM D256

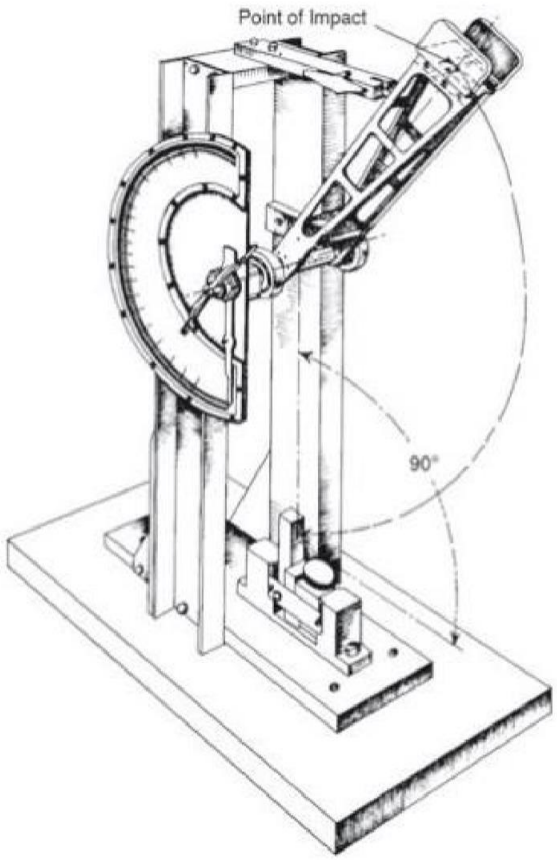

Figure 15 Cantilever Beam Izod Impact Machine [47]

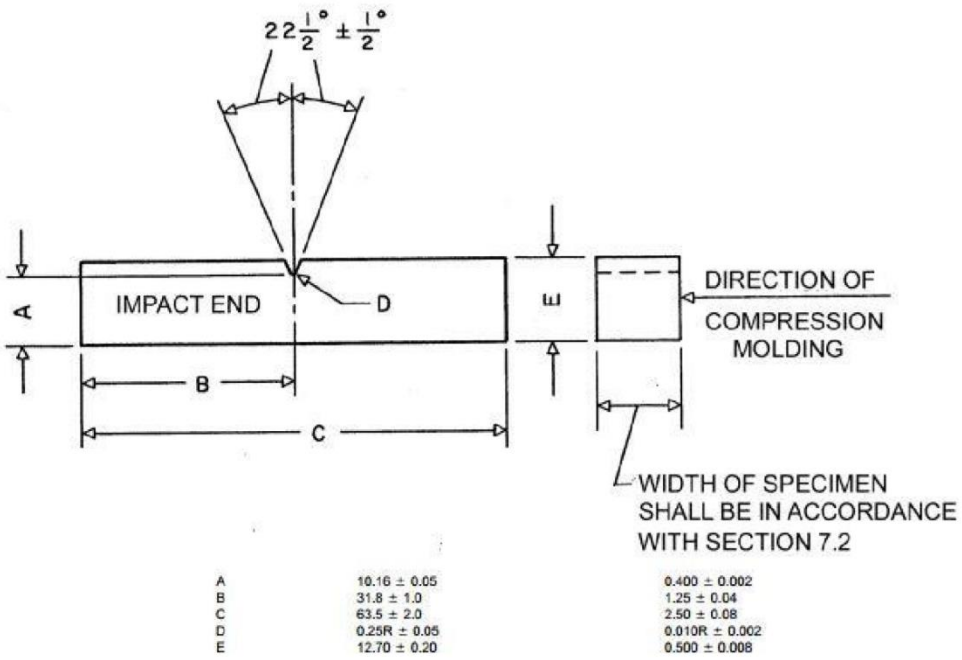

A	10.16 ± 0.05	0.400 ± 0.002
B	31.8 ± 1.0	1.25 ± 0.04
C	63.5 ± 2.0	2.50 ± 0.08
D	0.25R ± 0.05	0.010R ± 0.002
E	12.70 ± 0.20	0.500 ± 0.008

Figure 16 Dimensions of the Izod test specimen [47]

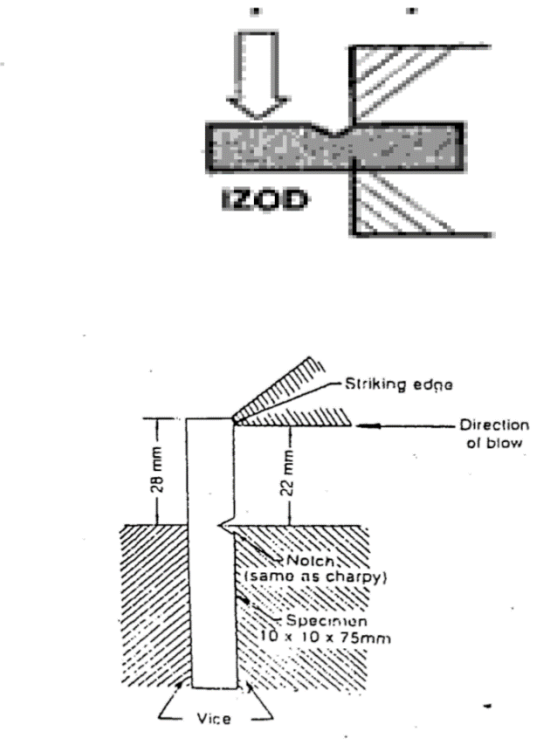

Figure 17 Position of Izod test specimen in the anvil [45]

2.12.2 SPECIMEN TYPE OF BREAKS

Different types of breaks occur in different specimens and one cannot compare impact data between two different types of breaks.

- Complete break (C) is a break where the specimen separates into two or more pieces.
- When the sample cannot support itself above the horizontal because the other part is held vertically about an angle less than 90^{o} included angle, a Hinge break (H) occurs.
- Partial break (P) is a type of an incomplete break when the sample has fractured/broken at least 90% of the distance between the vertex of the notch and the opposite side.
- Non-break (NB) is another type of incomplete break in which the fracture extends less than 90% of the distance between the vertex of the notch and the opposite side [47].

CHAPTER III

EQUIPMENT

3. 1 IMPACT TESTING MACHINE

The Izod test (ASTM D256) involves striking a specimen with a swinging hammer which is mounted at the end of the pendulum. The specimen is clamped vertically with the notch facing the striker. During the test, the striker swings down impacting the specimen. Sometimes, different sized strikers are used which imparts different amounts of energy to the specimen.

During impact, the striker has a known measure of kinetic energy. The impact energy is determined based on the height to which the striker would have risen, if no test specimen was set up, and this is contrasted with the height to which the striker actually rises when a specimen is present. The Izod impact test has a low strain rate. The impact test was carried out with an impact velocity of 3.5 m/s and at room temperature.

In this study, heavy weight (21.7 J) was used for testing of PEEK composites. The PEEK used in this study is solvay incorporated Ketaspire KT 820.

The samples were tested using an Instron Dynatup POE 2000 Impact tester, according to ASTM D256 shown in Fig. 18.

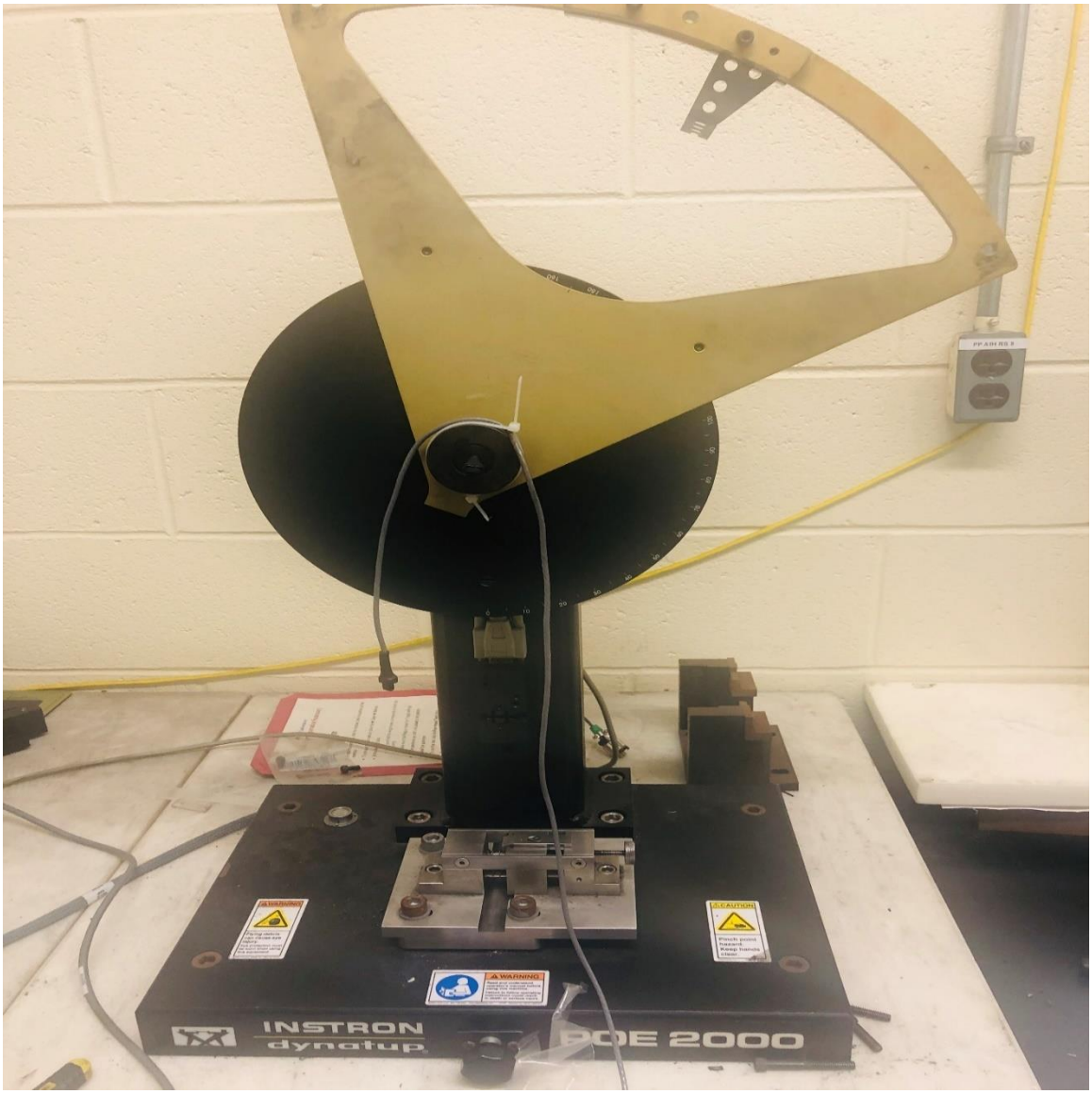

Figure 18 Instron Dynatup Impact testing machine.

3. 2 NOTCHER

The purpose of a notch is to make crack initiation easier and concentrate stresses which increases the probability of brittle fracture. It also controls the position at which the sample breaks.

A QUALITEST notcher was used to notch samples prior to Izod impact testing shown in Fig. 19. This notcher was used because the depth of the notch could be set prior to notching the sample and 5 or more samples could be notched at once.

Figure 19 Notcher.

3. 3 GOLD SPUTTER COATER

After the G-PMC samples were tested using the Izod impact test, the morphology of the fractured surfaces of the samples were viewed using SEM. Before this step, the samples were coated with a thin layer of conductive material in order to prevent the electrical charging of the surface. This also promotes the emission of secondary electrons. The addition of a thin layer of gold or gold-palladium alloy to the specimen through vacuum evaporation or sputter coating ensures that the specimen conducts evenly and delivers a homogeneous surface for analysis and imaging. Aluminium, silver and carbon can also be used to coat specimens but gold is the most widely used conductive metal coating because gold is an excellent conductor and it does not oxidize [50].

The fractured surfaces were mounted on aluminum studs, gold-coated to a thickness of 5nm using a EMS150T ES (Fig. 20) coater and placed under vacuum overnight prior to SEM.

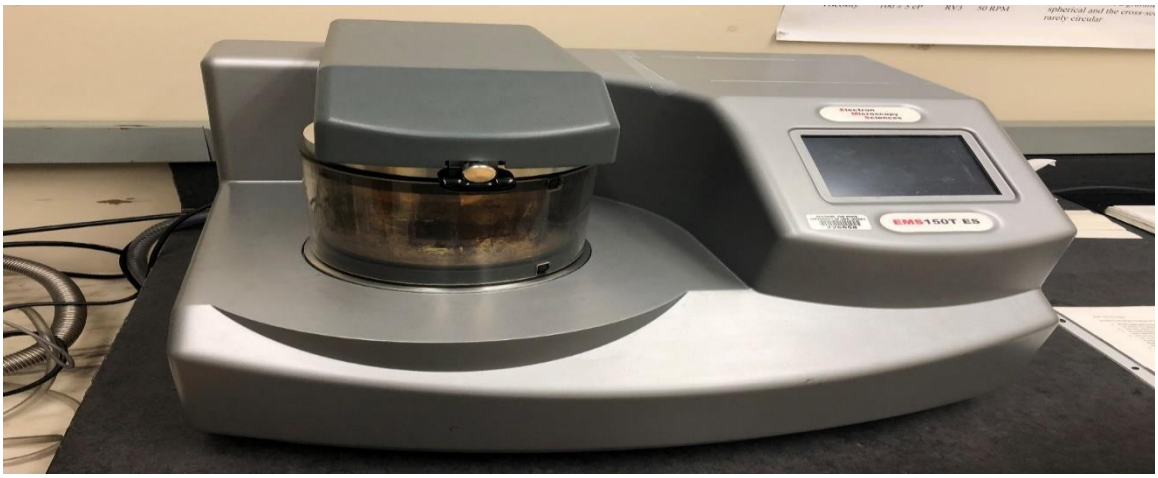

Figure 20 EMS150T ES Gold sputter coater.

3. 4 SCANNING ELECTRON MICROSCOPE

A scanning electron microscope (SEM) produces images of a specimen by scanning the surface with a focused beam of electrons. The electrons interact with the atoms present in the sample, producing many signals that contain information about the surface topography and composition of the sample. The electron beam scans the object in a raster scan pattern. The electrons which get reflected from the sample are captured by electron detectors, scanned and then imaged.

A Zeiss Sigma FESEM with Oxford EDS was used for the morphology analysis of the samples shown in Fig. 21.

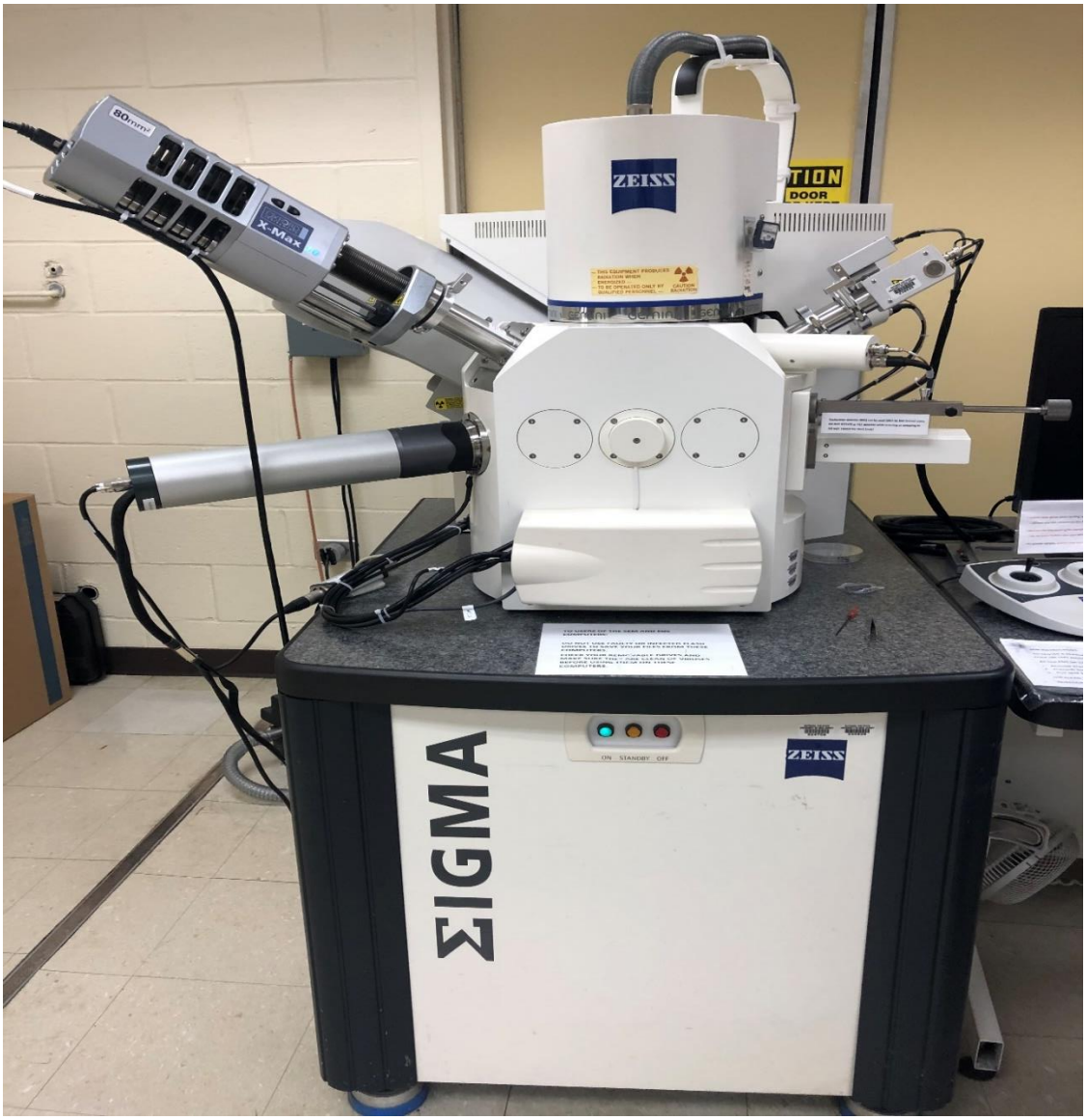

Figure 21 Zeiss Sigma FESEM.

CHAPTER IV

RESULTS AND DISCUSSIONS

PEEK, 2% G-PEEK and 35% G-PEEK were prepared using a modified single pass extruder process with three controlled heat zones. The PEEK samples were processed under a nitrogen blanket at 320 RPM with processing temperatures for zones 1,2,3 and the die, 670 ^{o}F, 690 ^{o}F, 695 ^{o}F, and 700 ^{o}F, respectively. The 2% G-PEEK samples were prepared under a nitrogen blanket at 370 RPM with processing temperatures for zones 1,2,3 and the die, 670 ^{o}F, 685 ^{o}F, 695 ^{o}F, and 700 ^{o}F respectively. The 35% G-PEEK samples were prepared under a nitrogen blanket at 320 RPM with processing temperatures for zones 1,2,3 and the die, 706 ^{o}F, 730 ^{o}F, 724 ^{o}F, and 741 ^{o}F respectively. The process to obtain fully exfoliated G-PMCs happens over a number of single pass cycles by in-situ exfoliation of graphite in the polymer matrix. As each processing cycle is complete, higher percentage of graphite is converted into graphene i.e. ratio of graphene to graphite increases.

The fractured surfaces of the neat PEEK and the composite samples were examined under the SEM and are illustrated below.

Fig. 22 shows the morphology of a fractured surface of Neat PEEK. Even at low magnifications, the charging of electrons is visible by the white areas on the Neat PEEK sample as shown in Fig. 22.

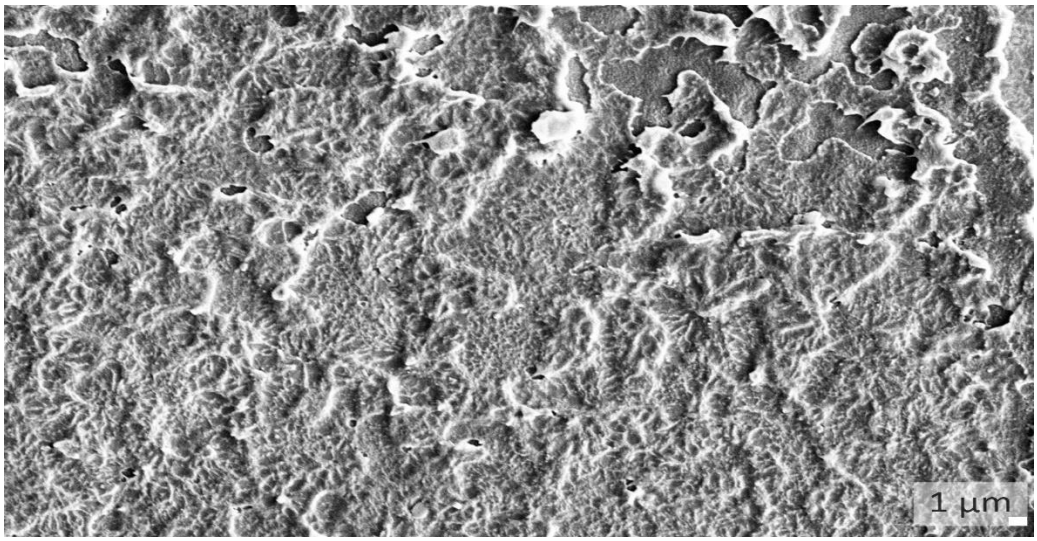

Figure 22 SEM image of Neat PEEK – Cycle 1.

Fig. 23 shows the morphology of a fractured surface of 2% G-PEEK – Cycle 1. We can see particles of intercalated graphite on the surface, as shown by the arrow. Fig. 24 shows the morphology of 2% G-PEEK – Cycle 3. We can notice much smaller pieces of graphite on the surface when compared to Cycle 1 and few pieces of graphene. Fig. 25 shows the morphology of 2% G-PEEK – Cycle 3 at higher magnification. A transparent layer of graphene is visible on the composite fracture surface as indicated by the arrow thus showing good graphene particle-matrix adhesion. We can also observe short pull-out lengths of polymer, as is evident by high-intensity charging and surface crystallization of PEEK. Fig. 26 shows the morphology of 2% G-PEEK - Cycle 5. The arrow in the figure corresponds to the graphene nanoflake particle. Many small ~10-micron graphene nanoflake particles and very few graphite particles are visible.

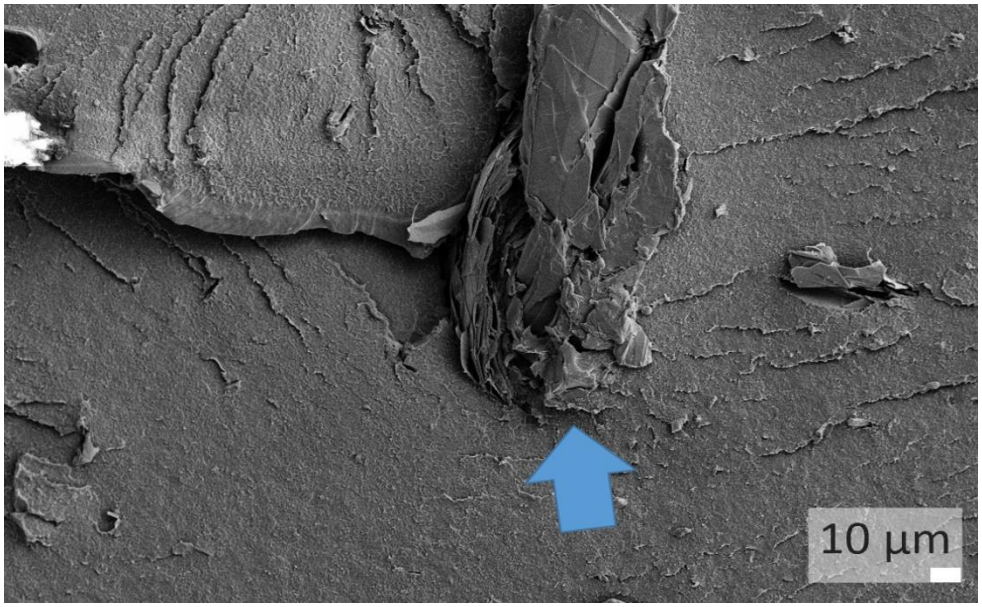

Figure 23 SEM image of 2% G-PEEK - Cycle 1, Graphite shown by arrow.

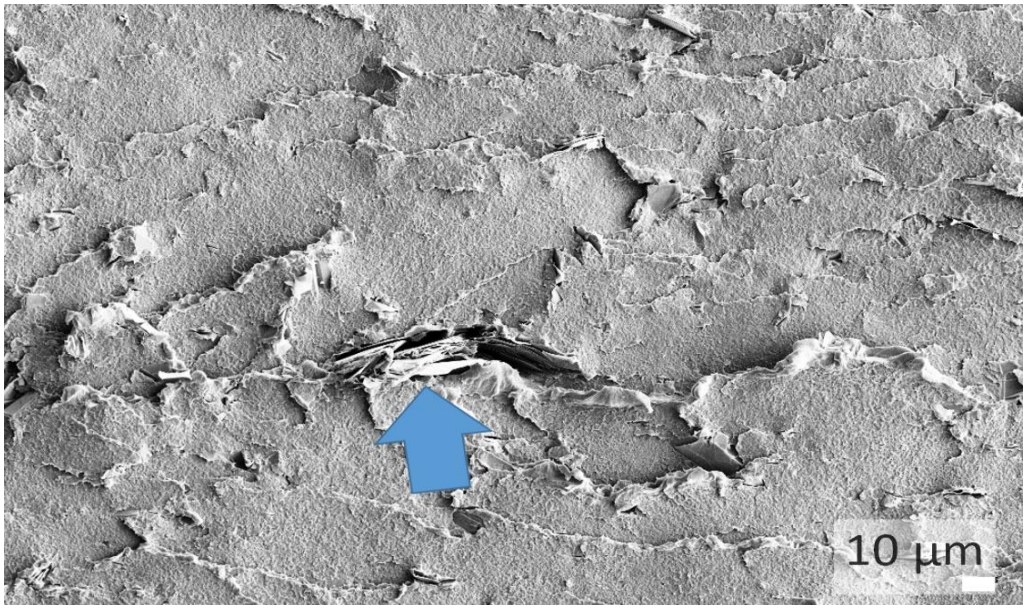

Figure 24 SEM image of 2% G-PEEK - Cycle 3, Graphite shown by arrow.

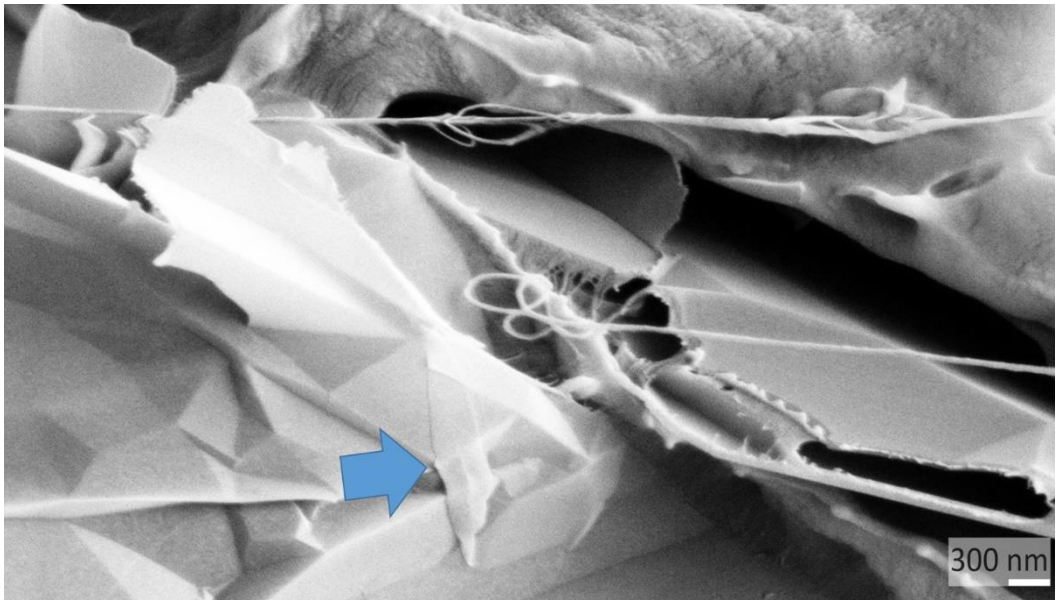

Figure 25 SEM image of 2% G-PEEK - Cycle 3, Higher Magnification.

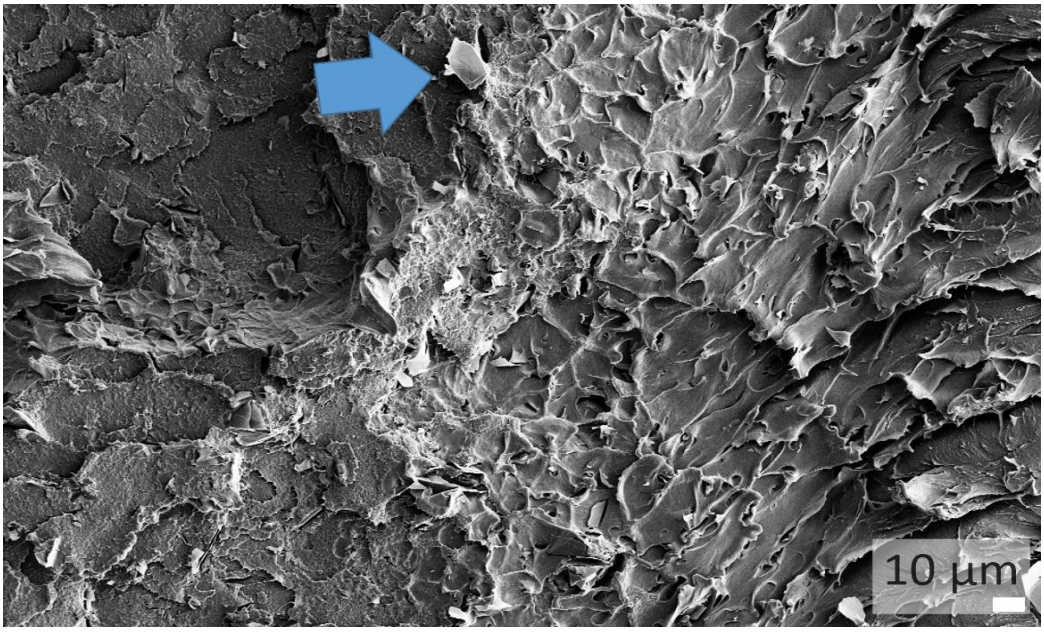

Figure 26 SEM image of 2% G-PEEK - Cycle 5, Graphene shown by arrow.

Fig. 27 shows the morphology of a fractured surface of 35% G-PEEK – Cycle 1. We can see particles of intercalated graphite on the surface, as shown by the arrow. Fig. 28 shows the morphology of 35% G-PEEK – Cycle 3. We can notice much smaller pieces of graphite on the surface when compared to Cycle 1 and few pieces of graphene. Fig. 29 shows the morphology of 35% G-PEEK - Cycle 5. We can see many small graphene nanoparticles and much smaller pieces of graphite as indicated by arrow. Comparing Fig. 22 to all the G-PEEK composite images, we can also see that the surface roughness increases when the amount of graphene increases.

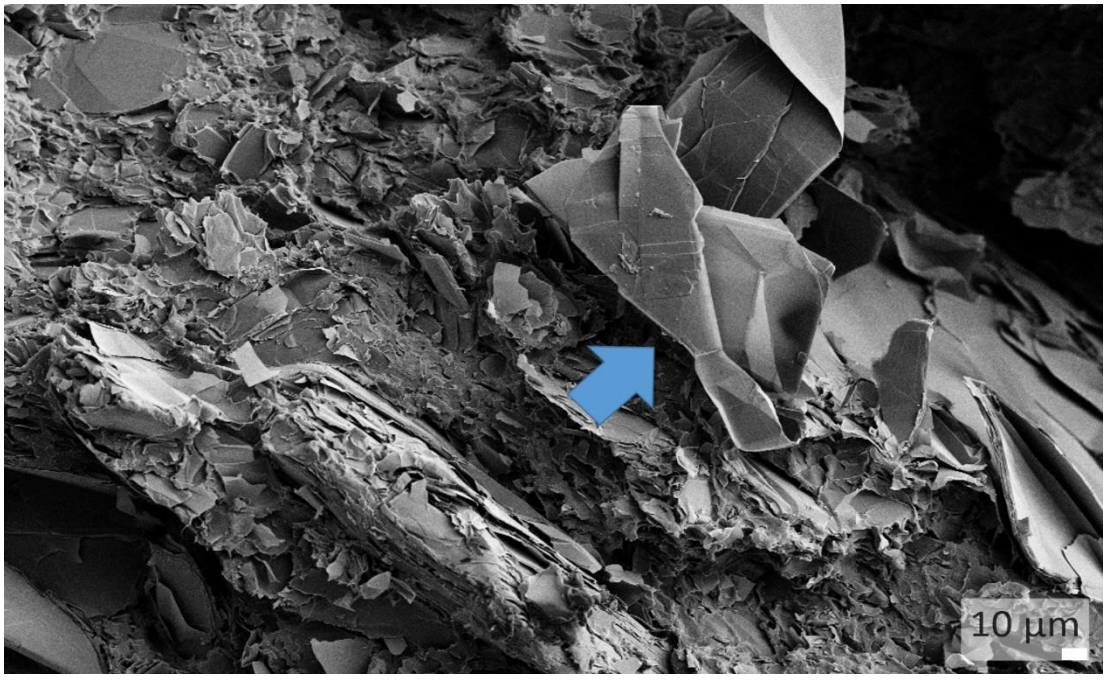

Figure 27 SEM image of 35% G-PEEK - Cycle 1, Graphite shown by arrow.

Figure 28 SEM image of 35% G-PEEK - Cycle 3, Graphite shown by arrow.

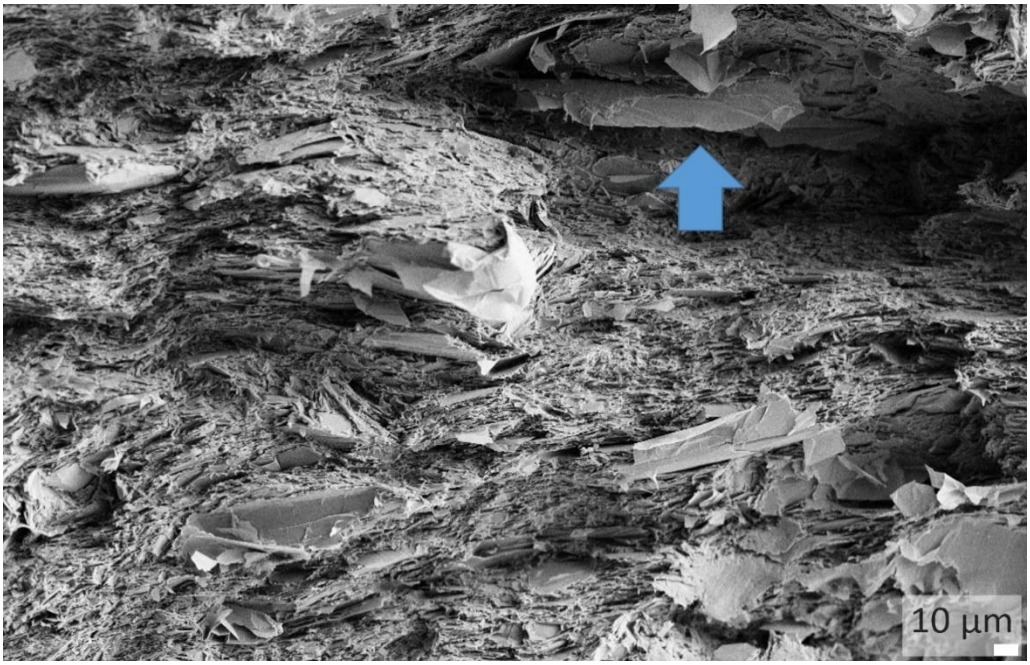

Figure 29 SEM image of 35% G-PEEK - Cycle 5, Graphite shown by arrow.

The published value of the impact energy of Neat PEEK – KT 820 is 9.2 kJ/m^2 [51]. The published value of the impact energy of PEEK KT 820 – CF30 (30% carbon fiber reinforced in PEEK) is 10 kJ/ m^2 [52]. Izod impact strength of 2% G-PEEK and 35% G-PEEK are shown in Fig. 30 and Fig. 31 respectively. All specimens in the composite samples underwent a complete break.

While comparing Fig. 30 and Fig. 31 we can see a similar trend. The impact energy of graphene reinforced PEEK is much higher than Neat PEEK and 30% Carbon fiber reinforced PEEK at all levels of exfoliations in both figures. We can also notice that with a higher percentage of graphite, which is represented at a low number of cycles, the impact strength is higher than medium number of cycles and goes back up again at a higher number of cycles when there is higher percentage of graphene present.

The Izod impact strength of 2% graphene reinforced PEEK is higher than that of Neat PEEK and 30% carbon fiber reinforced PEEK as shown in Fig. 30. The stiffness at 2% G-PEEK at any level of exfoliation remains same as Neat PEEK (3500 MPa) but the izod impact strength of 2% G-PEEK is much higher than that of Neat PEEK. As you can see from Fig. 30 and Fig. 31, the izod impact strength of 2% G-PEEK and 35% G-PEEK in all levels of exfoliation has increased compared to that of neat PEEK.

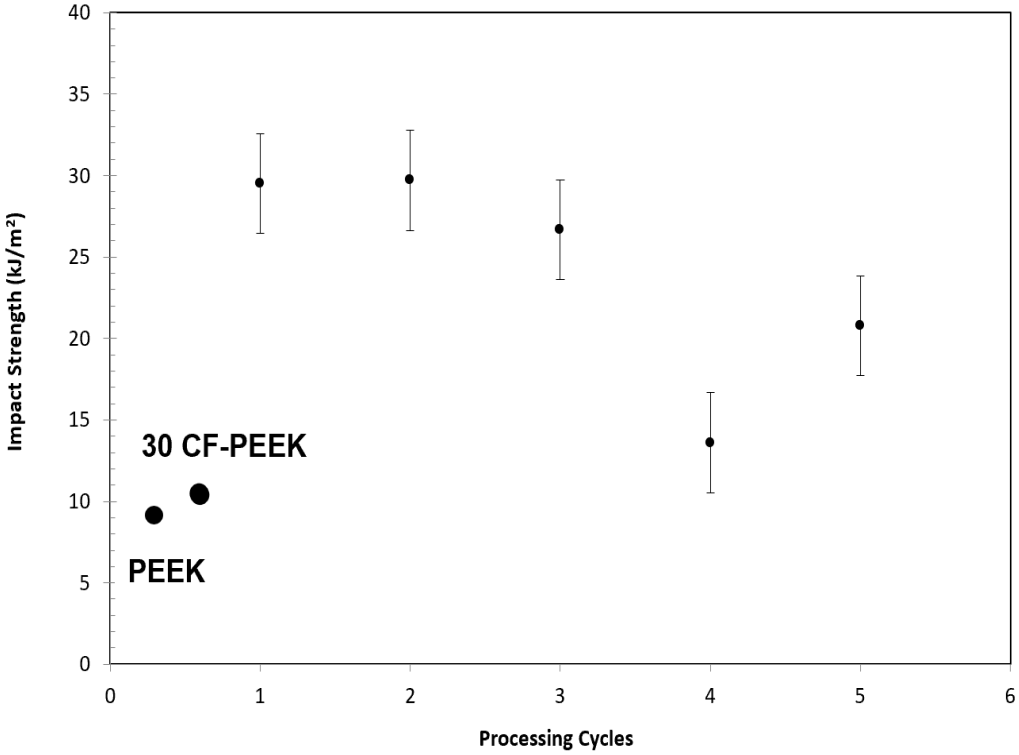

Figure 30 Notched impact strength of 2% G-PEEK.

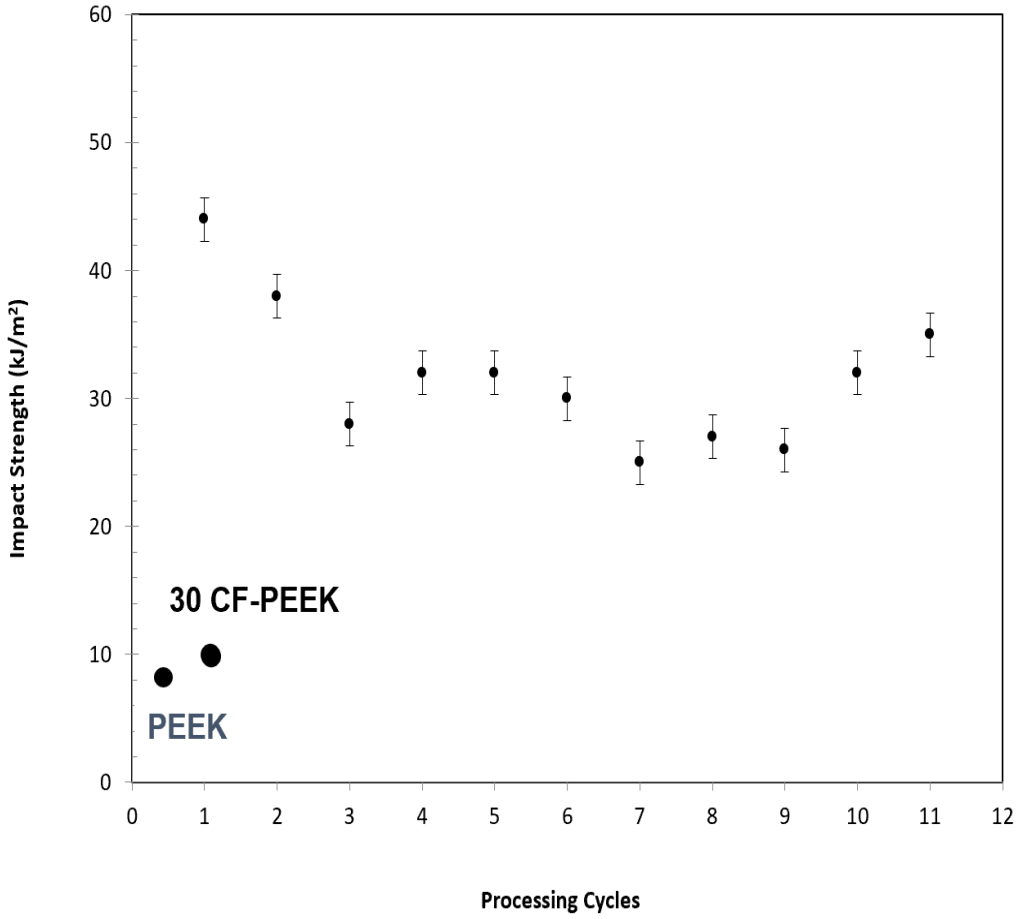

Figure 31 Notched impact strength of 35% G-PEEK.

Graphene-PEEK composites have low strain to failure as compared to Neat PEEK in a standard ASTM tensile test and low toughness, yet the impact strength increases. From Fig. 30 and Fig. 31, we can see that the impact strength of G-PEEK composites initially increases and then decreases and again increases, thus forming a U-shaped graph. This behavior may be explained by different ways which are discussed below.

When you push a pencil along a paper which signifies doing work, the graphite particle is sheared. The graphite particle can absorb a lot of energy when sheared apart by doing work and thus graphite is capable of absorbing a lot of impact energy prior to fracture. This effect is dominant when there is higher percentage of graphite present than graphene i.e. in the earlier processing cycles.

The polymer component is the only continuous phase in the polymer composite material. There is more opportunity to absorb moisture as the processing cycles increase and the plastic is heated longer thus degrading the plastic with time. This results in the decrease in the impact energy absorbed. We can notice that the impact strength reduces initially (both in Fig. 30 and Fig. 31) after each processing cycle which is the result of the degradation of the plastic.

The addition of graphene increases the impact strength because graphene inhibits crack propagation. When the amount of graphene present increases, the path for the crack to pass becomes really tortuous due to billion number of graphene plates. A bridging effect/blocking mechanism is created due to which the composite absorbs higher impact energy before fracture thus yielding higher impact strength materials. A lot of primary and secondary bonds are broken prior to fracture. This effect is dominant in the later cycles

when the impact strength again increases after initial few cycles which can be seen in both Fig. 30 and Fig. 31.

Thus, all the above-mentioned mechanisms explain the U-shaped graph. It should also be noted that the impact strength of the graphene reinforced PEEK is higher than that of Neat PEEK in all levels of exfoliations i.e. all processing cycles.

CHAPTER V

CONCLUSIONS

In this project, graphene-polymer matrix composites were prepared using high shear in-situ exfoliation of graphite in the polymer matrix. Graphene polymer composites with 2 wt.% graphene and 35 wt.% graphene was prepared. The impact strength and morphology of the fractured surfaces have been studied in this thesis. The fracture surfaces were examined by SEM to study the morphology of the composites. From the images, we can infer that as the amount of graphene increases the surface roughness also increases, thus increasing the impact strength of the composites. From the Izod impact testing results, we can conclude that the impact strength increases when the amount of graphene present increases. Further, the impact strength reduces with each processing cycle and then again increases leading to the formation of a U-shaped pattern.

Future investigations into a wider range of property testing to understand the effectiveness of in-situ shear processing, with a focus on assessing the response of various polymer chain chemistries to graphene produced by the in-situ shear process can be scope for future work. This will require the production and analysis of a greater number of graphite/graphene loadings, and over many degrees of exfoliation. Additionally, using mechanical, chemical, and structural analysis of the aforementioned composites, an effort can be undertaken to identify possible load transfer mechanisms.

CHAPTER VI

REFERENCES

[1] N. Lett, “Chapter 4 Electrical Properties of Graphene Wrinkles and Nanoribbons,” *Scanning*, pp. 41–68, 2009.

[2] T. Kuilla, S. Bhadra, D. Yao, N. H. Kim, S. Bose, and J. H. Lee, “Recent advances in graphene based polymer composites,” *Prog. Polym. Sci.*, vol. 35, no. 11, pp. 1350–1375, 2010.

[3] D. Verma, P. C. Gope, A. Shandilya, and A. Gupta, “Mechanical-Thermal-Electrical and Morphological Properties of Graphene Reinforced Polymer Composites: A Review,” *Trans. Indian Inst. Met.*, vol. 67, pp. 803–816, 2014.

[4] P. Sciences, “Characterisation of Graphene-Polymer Composites Yu-Chen Chang School of Materials,” 2012.

[5] P. Alexandre, M. and Dubois, “No Title,” *Polym. Silic. nanocomposites Prep. Prop. uses a new Cl. Mater. Mater. Sci. Eng. R Reports, 28(1-2) 1-63*, 2000.

[6] B. W. Station and J. Washington, “Graphene-reinforced polymer matrix composites,” vol. 10329391, pp. 1–23, 2020.

[7] U. Khan, P. May, A. O’Neill, and J. N. Coleman, “Development of stiff, strong, yet tough composites by the addition of solvent exfoliated graphene to polyurethane,” *Carbon N. Y.*, vol. 48, no. 14, pp. 4035–4041, 2010.

[8] G. Romhány and G. Szebényi, “Interlaminar crack propagation in MWCNT/fiber reinforced hybrid composites,” *Express Polym. Lett.*, vol. 3, no. 3, pp. 145–151, 2009.

[9] K. Kalaitzidou, H. Fukushima, and L. T. Drzal, “Mechanical properties and morphological characterization of exfoliated graphite-polypropylene nanocomposites,” *Compos. Part A Appl. Sci. Manuf.*, vol. 38, no. 7, pp. 1675–1682, 2007.

[10] A. Tewatia, J. Hendrix, T. Nosker, and J. Lynch-Branzoi, “Multi-scale carbon (micro/nano) fiber reinforcement of polyetheretherketone using high shear melt-processing,” *Fibers*, vol. 5, no. 3, 2017.

[11] D. R. Paul and L. M. Robeson, “Polymer nanotechnology: Nanocomposites,” *Polymer (Guildf).*, vol. 49, no. 15, pp. 3187–3204, 2008.

[12] X. X. Chu, Z. X. Wu, R. J. Huang, Y. Zhou, and L. F. Li, “Mechanical and thermal expansion properties of glass fibers reinforced PEEK composites at cryogenic temperatures,” *Cryogenics (Guildf).*, vol. 50, no. 2, pp. 84–88, 2010.

[13] Y. Lee and R. S. Porter, “Crystallization of PEEK in Carbon Fiber Composites,”

Polym. Eng. Sci., vol. 26, no. 1 5, pp. 633–639, 1986.

[14] A. C. Martin *et al.*, "Amorphous-to-crystalline transition of Polyetheretherketone-carbon nanotube composites via resistive heating," *Compos. Sci. Technol.*, vol. 89, pp. 110–119, 2013.

[15] A. M. Díez-Pascual *et al.*, "Development and characterization of PEEK/carbon nanotube composites," *Carbon N. Y.*, vol. 47, no. 13, pp. 3079–3090, 2009.

[16] D. S. Bangarusampath, H. Ruckdäschel, V. Altstädt, J. K. W. Sandler, D. Garray, and M. S. P. Shaffer, "Rheology and properties of melt-processed poly(ether ether ketone)/multi-wall carbon nanotube composites," *Polymer (Guildf).*, vol. 50, no. 24, pp. 5803–5811, 2009.

[17] S. Sinha Ray and M. Okamoto, "Polymer/layered silicate nanocomposites: A review from preparation to processing," *Prog. Polym. Sci.*, vol. 28, no. 11, pp. 1539–1641, 2003.

[18] X. Zhang, J. Zheng, and Z. Ma, "Graphene-polymer Composites for Enhancing the Mechanical Properties," *IOP Conf. Ser. Mater. Sci. Eng.*, vol. 538, no. 1, 2019.

[19] K. Hu, D. D. Kulkarni, I. Choi, and V. V. Tsukruk, "Graphene-polymer nanocomposites for structural and functional applications," *Prog. Polym. Sci.*, vol. 39, no. 11, pp. 1934–1972, 2014.

[20] L. Tang, L. Zhao, and L. Guan, "7 Graphene / Polymer Composite Materials : Processing , Properties and Applications."

[21] A. K. Geim and K. S. Novoselov, "The rise of graphene," *Nat. Mater.*, vol. 6, no. 3, pp. 183–191, 2007.

[22] M. M. Hossain, "Review The Fate of Graphene in Biomedical Applications," pp. 1–13, 2019.

[23] et al. Lee, C., Wei, X., Kysar, J.W., "No Title," *"Measurement Monolayer, elastic Prop. intrinsic strength graphene," Sci. 321 385-388.*, 2008.

[24] A. A. Balandin *et al.*, "Superior thermal conductivity of single-layer graphene," *Nano Lett.*, vol. 8, no. 3, pp. 902–907, 2008.

[25] X. Du, I. Skachko, A. Barker, and E. Y. Andrei, "Approaching ballistic transport in suspended graphene," *Nat. Nanotechnol.*, vol. 3, no. 8, pp. 491–495, 2008.

[26] U. E. Paulista, P. D. E. P. Em, and C. Biológicas, "Development of Nanocomposites by Graphene Synthesized by Solvent Exfoliation Method," no. December 2014.

[27] H. Kim, A. A. Abdala, and C. W. MacOsko, "Graphene/polymer nanocomposites," *Macromolecules*, vol. 43, no. 16, pp. 6515–6530, 2010.

[28] N. Pan, "Analytical Characterization of the Anisotropy and Local Heterogeneity of Short Fiber Composites: Fiber Fraction as a Variable," *J. Compos. Mater.*, vol. 28, no. 16, pp. 1500–1531, 1994.

[29] D. Haasenritter, “and Publications,” *Correct. Today*, vol. 17, no. December, pp. 8–15, 2008.

[30] Prateek, V. K. Thakur, and R. K. Gupta, “Recent Progress on Ferroelectric Polymer-Based Nanocomposites for High Energy Density Capacitors: Synthesis, Dielectric Properties, and Future Aspects,” *Chem. Rev.*, vol. 116, no. 7, pp. 4260–4317, 2016.

[31] Y. Kojima, A. Usuki, M. Kawasumi, A. Okada, T. Kurauchi, and O. Kamigaito, “Synthesis of nylon 6–clay hybrid by montmorillonite intercalated with ϵ-caprolactam,” *J. Polym. Sci. Part A Polym. Chem.*, vol. 31, no. 4, pp. 983–986, 1993.

[32] S. Stankovich *et al.*, “Graphene-based composite materials,” *Nature*, vol. 442, no. 7100, pp. 282–286, 2006.

[33] W. Li, A. Dichiara, and J. Bai, “Carbon nanotube-graphene nanoplatelet hybrids as high-performance multifunctional reinforcements in epoxy composites,” *Compos. Sci. Technol.*, vol. 74, pp. 221–227, 2013.

[34] D. D. Kulkarni, I. Choi, S. S. Singamaneni, and V. V. Tsukruk, “Graphene oxide - Polyelectrolyte nanomembranes,” *ACS Nano*, vol. 4, no. 8, pp. 4667–4676, 2010.

[35] et al. Lahiri, D., Das, S., Choi, W., “No Title,” *“Unfolding The, damping Behav. multilayer graphene Membr. low-frequency regime,” ACS Nano, 6 3992–4000.*, 2012.

[36] H. Fischer, “Polymer nanocomposites: From fundamental research to specific applications,” *Mater. Sci. Eng. C*, vol. 23, no. 6–8, pp. 763–772, 2003.

[37] Alhajji and Eman Mousa, “The effects of strengthening mechanisms and time rating on the mechanical properties of metals and polymers using Tensile tests,” 2016.

[38] D. Galpaya, “Synthesis, Characterization and Application of Graphene-Oxide Polymer Composites,” no. June, pp. 1–195, 2015.

[39] J. R. Potts, S. Murali, Y. Zhu, X. Zhao, and R. S. Ruoff, “Microwave-exfoliated graphite oxide/polycarbonate composites,” *Macromolecules*, vol. 44, no. 16, pp. 6488–6495, 2011.

[40] H. C. Schniepp *et al.*, “Functionalized single graphene sheets derived from splitting graphite oxide,” *J. Phys. Chem. B*, vol. 110, no. 17, pp. 8535–8539, 2006.

[41] M. Naebe *et al.*, “Mechanical Property and Structure of Covalent Functionalised Graphene/Epoxy Nanocomposites,” *Sci. Rep.*, vol. 4, pp. 1–7, 2014.

[42] O. C. Compton, S. Kim, C. Pierre, J. M. Torkelson, and S. T. Nguyen, “Crumpled graphene nanosheets as highly effective barrier property enhancers,” *Adv. Mater.*, vol. 22, no. 42, pp. 4759–4763, 2010.

[43] B. Unnikrishnan, S. Palanisamy, and S. M. Chen, “A simple electrochemical

approach to fabricate a glucose biosensor based on graphene-glucose oxidase biocomposite," *Biosens. Bioelectron.*, vol. 39, no. 1, pp. 70–75, 2013.

[44] "The History of Instrumented Impact Testing M. P. Manahan* and T. A. Siewert**."

[45] N.Singh, "Experimental Study and Parametric Design of Impact Testing Methodology," no. June, pp. 1–76, 2009.

[46] A. Naranjo, M. del Pilar Noriega E., T. A. Osswald, A. Roldán-Alzate, and J. D. Sierra, "Plastics Testing and Characterization," *Plast. Test. Charact.*, 2008.

[47] American Society for Testing & Mater, "Standard test methods for felt," no. June 2004, pp. 1–20, 1987.

[48] AZoM, "Charpy test : Determination of impact energy using the charpy test," *Azo Mater.*, pp. 1–4, 2005.

[49] I. Mugenyi and I. Mugenyi, "Impact strength testing device," 2019.

[50] S. A. Leslie and J. C. Mitchell, "Removing gold coating from sem samples," *Palaeontology*, vol. 50, no. 6, pp. 1459–1461, 2007.

[51] T. D. Sheet, "KetaSpire ® KT-820," pp. 1–5, 2015.

[52] K. K.- Cf, "KetaSpire ® KT-820 CF30," pp. 4–7, 2013.